SUPPORTING INFORMATION

Design of task-specific fluorinated ionic liquids: nanosegregation versus hydrogen-bonding ability in aqueous solutions

Joana C. Bastos,[a] Sara F. Carvalho,[a] Tom Welton,[b] José N. Canongia Lopes,[c] Luís Paulo N. Rebelo,[a] Karina Shimizu,[c] João M. M. Araújo[a,*] and Ana B. Pereiro[a,*]

[a] LAQV, REQUIMTE, Departamento de Química, Faculdade de Ciências e Tecnologia, Universidade Nova de Lisboa, 2829-516, Caparica, Portugal

[b] Department of Chemistry, Imperial College London, Exhibition Road, London, UK SW7 2AY

[c] Centro de Química Estrutural, IST/UTL, 1049-001 Lisboa, Portugal

*Corresponding Author: jmmda@fct.unl.pt (J. M. M. Araújo) and anab@fct.unl.pt (A.B. Pereiro)

Experimental Section

Materials

1-Ethyl-3-methylimidazolium acetate, $[C_2C_1Im][C_1CO_2]$, > 95 % mass faction purity; 1-ethyl-3-methylimidazolium methanesulfonate, $[C_2C_1Im][C_1SO_3]$, ≥ 99% mass fraction purity; 1-ethyl-3-methylimidazolium trifluoroacetate, $[C_2C_1Im][CF_3CO_2]$, ≥ 97% mass fraction purity; 1-ethyl-3-methylimidazolium trifluoromethanesulfonate, $[C_2C_1Im][CF_3SO_3]$, ≥ 99% mass fraction purity; 1-ethyl-3-methylimidazolium 1,1,2,2-tetrafluoroethanesulfonate, $[C_2C_1Im][C_2F_4SO_3]$, ≥ 98% mass fraction purity; 1-ethyl-3-methylimidazolium perfluorobutanesulfonate, $[C_2C_1Im][C_4F_9SO_3]$, >97% mass fraction purity; 1-ethyl-3-methylimidazolium perfluorooctanesulfonate, $[C_2C_1Im][C_8F_{17}SO_3]$, > 98% mass fraction purity; 1-butyl-3-methylimidazolium trifluoromethanesulfonate, $[C_4C_1Im][CF_3SO_3]$, ≥ 99% mass faction purity and 1-butyl-3-methylimidazolium bis(trifluoromethylsulfonyl)imide, $[C_4C_1Im][NTf_2]$, ≥ 99% mass faction purity, were acquired at IoLiTec. The purity of all ionic liquids was verified by ^{1}H and ^{19}F NMR. Previously to any use, all samples were dried under a $3·10^{-2}$ Torr vacuum and vigorous stirring for at least 48 hours to avoid volatile impurities. Acetate-based ILs were maintained at 313.15 K and the remaining ILs at 323.15 K. Then, water content was determined using Karl Fischer coulometric titration method (Metrohm 831 KF Coulometer) and it was less than 100 ppm. The structures and acronyms of the ionic liquids are listed in Table S1.

In order to characterize the polarity by the Kamlet-Taft method, three dyes were used: 4-Nitroanliline, ≥99% mass fraction purity acquired at Fluka; N-N-diethyl-4-nitroaniline, ≥97% mass fraction purity acquired at Fluorochem Ltd.; and 2,6-Diphenyl-4-(2,4,6-triphenyl-1-pyridinio)phenolate, also known as Reichardt's dye, with 90% mass fraction purity acquired at Sigma-Aldrich. Dichloromethane, ≥ 99.9% mass fraction purity acquired at Sigma-Aldrich, was used to dilute the dyes and Milli-Q ultrapure water (Milli-Q Integral Water Purification System) to dilute the samples.
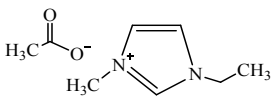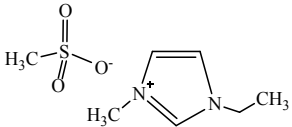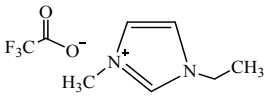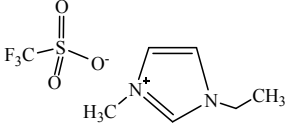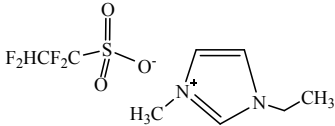
Dye Solutions and Samples Preparation

The stock solutions of 4-nitroanliline, N,N-diethyl-4-nitroaniline and Reichardt's dye were prepared using ± 0.010 g of dye in a glass vial and mixed with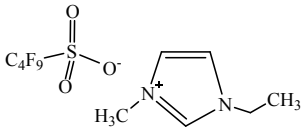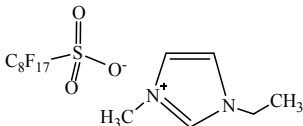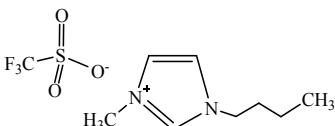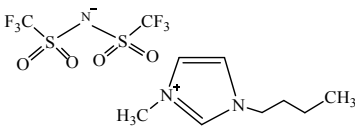 10 mL of dichloromethane (DCM). An additional 1:10 dilution with DCM was made in the case of 4-nitroanliline and N,N-diethyl-4-nitroaniline to ensure an absorbance less than 1.2. All the stock solutions were previously maintained at 277 K after their preparation to avoid DCM evaporation.

Roughly 0.34 mL of 4-nitroanliline and N-N-diethyl-4-nitroaniline and 1.3 mL of Reichardt's dye were added to a glass vial with an open top screw-caped sealed with a silicone septum. To remove the DCM from dye solutions, samples were submitted to a $3·10^{-2}$ Torr vacuum at room-temperature for at least 30 minutes. In order to prevent leakages in such extreme vacuum conditions, a 0.8 x 30 mm regular needle was slightly skewered in to the silicone septum. Thus, 0.4 mg of sample is added to the vial and vigorously stirred in a vortex until all blended.

For neat ionic liquids measurements, samples were directly added to the dyes. To evaluate the water effect, 1.6 mL of ionic liquid aqueous solution was prepared in a clear glass vial using Milli-Q water. The different IL concentrations were prepared by weighting the ionic liquid and the Milli-Q water at fixed weight fractions. The range of concentrations varied from 100 wt% to 30 wt%, except for $[C_2C_1Im][C_8F_{17}SO_3]$ where the range concentration varied from 45 wt% to 30 wt%. This FIL is solid at room temperature (melting point = 367.72 K)[S1] and the Kamelt-Taft parameters at high concentrations was impossible to determine (turbidity problems) due to their high surfactant power and viscosity.[S2]

**Table S1** Description of the ionic liquids and inorganic salts used in this work.

Formal Name	Structure	Abbreviation
1-Ethyl-3-methylimidazolium acetate		$[C_2C_1Im][C_1CO_2]$
1-Ethyl-3-methylimidazolium methanesulfonate		$[C_2C_1Im][C_1SO_3]$
1-Ethyl-3-methylimidazolium trifluoroacetate		$[C_2C_1Im][C_1F_3CO_2]$
1-Ethyl-3-methylimidazolium trifluoromethanesulfonate		$[C_2C_1Im][C_1F_3SO_3]$
1-Ethyl-3-methylimidazolium 1,1,2,2-tetrafluoroethanesulfonate		$[C_2C_1Im][C_2F_4SO_3]$
1-Ethyl-3-methylimidazolium perfluorobutanesulfonate		$[C_2C_1Im][C_4F_9SO_3]$
1-Ethyl-3-methylimidazolium perfluorooctanesulfonate		$[C_2C_1Im][C_8F_{17}SO_3]$
1-Butyl-3-methylimidazolium trifluoromethanesulfonate		$[C_4C_1Im][C_1F_3SO_3]$
1-Butyl-3-methylimidazolium bis(trifluoromethylsulfonyl)imide		$[C_4C_1Im][NTf_2]$

Dye Solutions and Samples Preparation

Kamlet-Taft solvatochromic parameters were obtained using an UV-Vis VWR® spectrophotometer, model UV-6300PC. Each sample was loaded into a dry cuvette and measured in a scan range of 250 to 800 nm at 100.00 nm/min. In order to obtain a high spectra resolution, a 0.1 nm interval was chosen. The spectrum for each sample was recorded three times and the wavelengths in which the absorbance was maximum were acquired. All spectra were analysed using the UV-Vis Analyst Software.

Validation of Experimental Procedure

The experimental procedure used in this work was validated using conventional ionic liquids (1-butyl-3-methylimidazolium bis(trifluoromethylsulfonyl)imide, $[C_4C_1Im][NTf_2]$, and 1-butyl-3-methylimidazolium perfluoromethanesulfonate, $[C_4C_1Im][C_1F_3SO_3])$[S3] as you can see in Fig. S1.
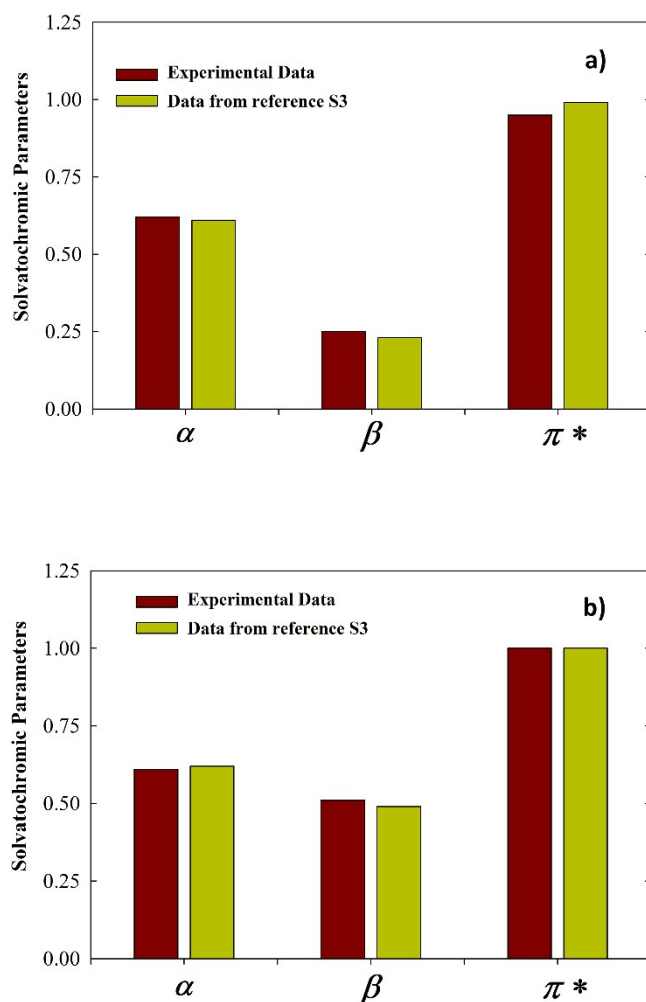

Fig. S1 Comparison between experimental and literature data (from reference S3) of Kamlet-Taft parameters for traditional ionic liquids at 298.15 K: a) 1-butyl-3-methylimidazolium bis(trifluoromethylsulfonyl)imide, $[C_4C_1Im][NTf_2]$; and b) 1-butyl-3-methylimidazolium perfluoromethanesulfonate, $[C_4C_1Im][C_1F_3SO_3]$.

Kamlet-Taft Parameters of IL + H₂O Systems
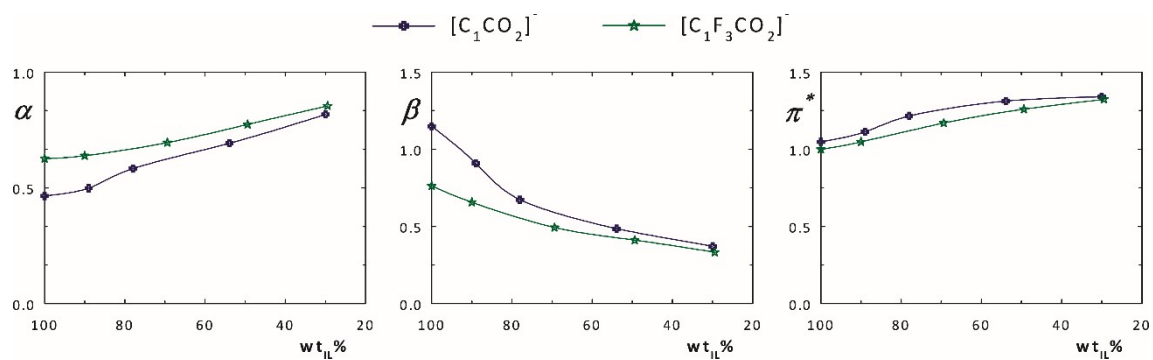
Fig. S2 Kamlet-Taft parameters (dye set Reichardt's dye, N,N-diethyl-4-nitroaniline and 4-nitroanliline) for the binary systems $[C_2C_1Im][RCO_2]$ + H_2O at 298.15 K.
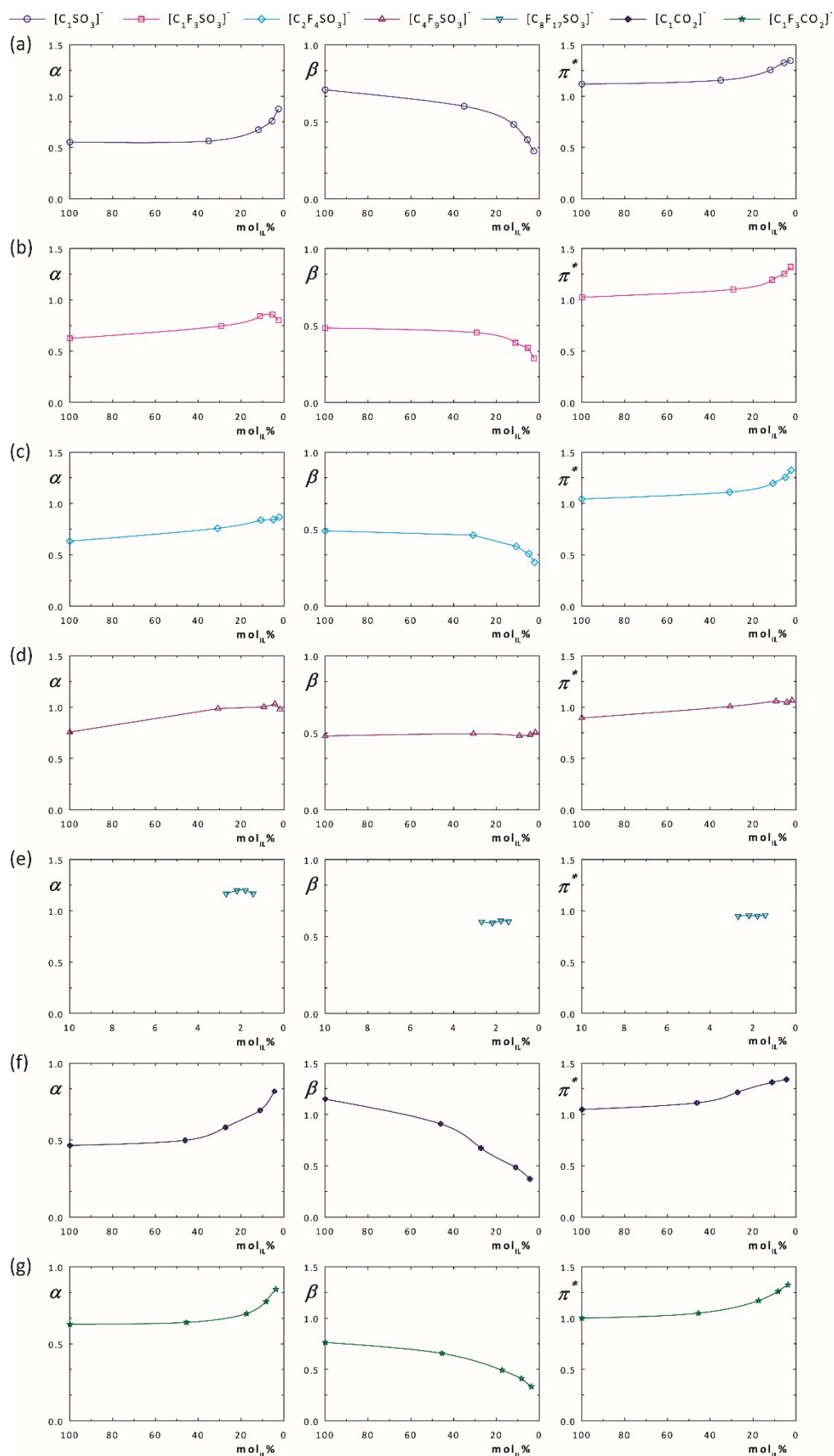
Fig. S3 Kamlet-Taft parameters (dye set Reichardt's dye, N,N-diethyl-4-nitroaniline and 4-nitroanliline) for the binary systems $[C_2C_1Im][RSO_3]$ + H_2O (a–e) and $[C_2C_1Im][RCO_2]$ + H_2O (f, g) at 298.15 K, expressed in $mol_{IL}\%$.

5
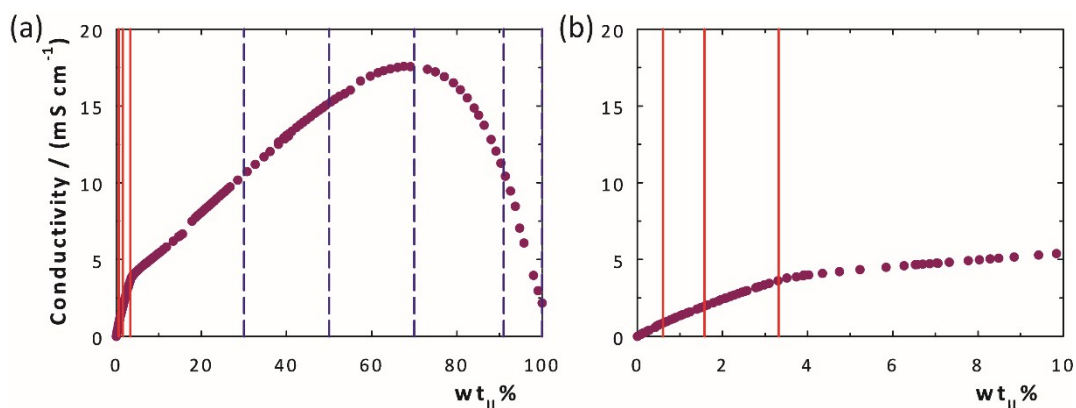
Fig. S4 Electrical conductivity profile of $[C_2C_1Im][C_4F_9SO_3] + H_2O$ system at 298.15 K. The three critical aggregation concentrations (solid red lines) and the herein studied FIL concentrations in wt% (dashed blue lines) are also depicted. a) full concentration range and b) inset. Data adapted from reference S4.
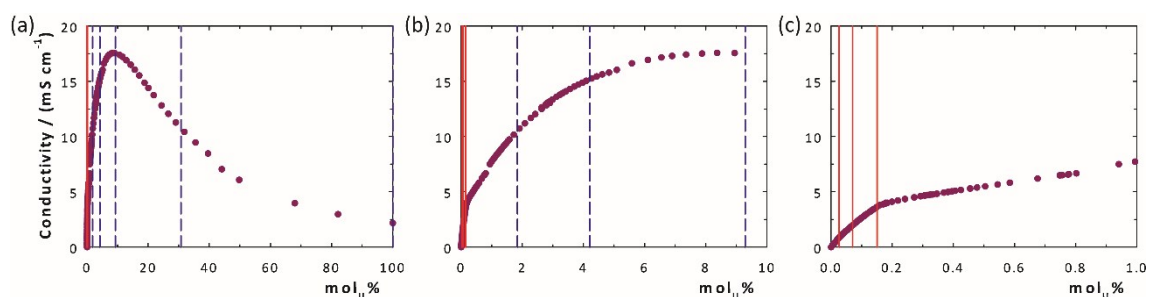
Fig. S5 Electrical conductivity profile of $[C_2C_1Im][C_4F_9SO_3] + H_2O$ system at 298.15 K. The three critical aggregation concentrations (solid red lines) and the herein studied FIL concentrations in mol% (dashed blue lines) are also depicted. a) full concentration range and b, c) inset. Data adapted from reference S4.

Table S2 Kamlet-Taft parameters, hydrogen-bond donor (α), hydrogen-bond acceptor (β), and dipolarity/polarizability (π^*), with their corresponding standards deviations (σ), determined for the neat ILs and aqueous solutions studied in this work.

IL wt%	$\alpha \pm \sigma$	$\beta \pm \sigma$	$\pi^* \pm \sigma$	IL wt%	$\alpha \pm \sigma$	$\beta \pm \sigma$	$\pi^* \pm \sigma$	IL wt%	$\alpha \pm \sigma$	$\beta \pm \sigma$	$\pi^* \pm \sigma$
	$[C_2C_1Im][C_1CO_2]$				$[C_2C_1Im][C_1SO_3]$				$[C_2C_1Im][C_1F_3CO_2]$		
100	0.465 ±0.001	1.15 ±0.040	1.05 ±0.002	100	0.552 ±0.004	0.708±0.012	1.12 ±0.005	100	0.627 ±0.002	0.762 ±0.001	1.00 ±0.002
89	0.499 ±0.002	0.909 ±0.001	1.11 ±0.001	90	0.562 ±0.001	0.601 ±0.002	1.15 ±0.002	90	0.639 ±0.001	0.656 ±0.002	1.05 ±0.002
78	0.583 ±0.002	0.672 ±0.004	1.22 ±0.002	69	0.672 ±0.004	0.483 ±0.001	1.25 ±0.001	69	0.695 ±0.001	0.492 ±0.005	1.17 ±0.001
56	0.692 0.001	0.485 ±0.007	1.31 ±0.001	49	0.756 ±0.001	0.383 ±0.007	1.32 ±0.001	49	0.774 ±0.008	0.411 ±0.003	1.26 ±0.001
30	0.817 ±0.001	0.370 ±0.016	1.34 ±0.001	30	0.874 ±0.001	0.310 ±0.014	1.35 ±0.012	29	0.854 ±0.004	0.332 ±0.001	1.32 ±0.001
	$[C_2C_1Im][C_1F_3SO_3]$				$[C_2C_1Im][C_2F_4SO_3]$				$[C_2C_1Im][C_4F_9SO_3]$		
100	0.623 ± 0.022	0.484 ±0.006	1.02 ±0.001	100	0.632 ±0.002	0.489 ±0.001	1.04 ±0.002	100	0.757 ±0.001	0.479 ±0.006	0.894 ±0.001
88	0.745 ±0.013	0.454 ±0.031	1.10 ±0.018	90	0.758 ±0.001	0.461 ±0.006	1.11 ±0.003	91	0.986 ±0.001	0.494 ±0.007	1.01 ±0.001
69	0.840 ±0.005	0.388 ± 0.014	1.19 ±0.004	69	0.837 ±0.013	0.387 ±0.006	1.20 ±0.003	70	1.00 ±0.011	0.482 ±0.022	1.06 ±0.002
50	0.855 ±0.002	0.355 ±0.007	1.25 ±0.001	50	0.843 ±0.002	0.340 ±0.001	1.25 ±0.001	50	1.03 ±0.004	0.488 ±0.006	1.05 ±0.006
31	0.801 ±0.005	0.286 ±0.002	1.32 ±0.001	30	0.865 ±0.001	0.284 ±0.001	1.32 ±0.001	30	0.979 ±0.017	0.502 ±0.038	1.06 ±0.019
	$[C_2C_1Im][C_8F_{17}SO_3]$				Water						
45	1.17 ±0.006	0.596 ±0.009	0.947 ±0.001	0[a]	1.11 ±0.002	0.130 ±0.014	1.34 ±0.001				
40	1.20 ±0.002	0.588 ±0.007	0.954 ±0.003		(1.12)[b]	(0.14)[b]	(1.33)[b]				
35	1.20 ±0.001	0.602 ±0.002	0.949 ±0.002		(1.02-1.17)[c]	(0.14-0.18)[c]	(1.09)[c]				
30	1.17 ±0.003	0.597 ±0.006	0.956 ±0.003		(1.17)[d]	(0.17)[d]	(1.09)[d]				

[a] Milli-Q ultrapure water
[b] data from reference S5
[c] data from reference S6
[d] data from reference S7

Molecular Dynamics Simulations.

The atomistic description of water, and the $[C_2C_1Im][C_1F_3SO_3]$, $[C_2C_1Im][C_2F_4SO_3]$, $[C_2C_1Im][C_4F_9SO_3]$, $[C_2C_1Im][C_8F_{17}SO_3]$, $[C_2C_1Im][C_1SO_3]$, $[C_2C_1Im][C_4H_9SO_3]$, $[C_2C_1Im][C_1CO_2]$ and $[C_2C_1Im][C_1F_3CO_2]$ ionic liquids was implemented using the SPC,[S8] and CL&P[S9-S11] force-fields, respectively. The MD simulations were carried out using the DL_POLY 2.20[S12] and Gromacs[S13-S15] packages.

The runs in DL_POLY (systems 1 to 24 in Table S3) started from low-density configurations built with the PACKMOL package[S16] and were performed using 2 fs timesteps and 2 nm cutoff distances. All simulations were subjected to equilibration runs under isobaric isothermal ensemble conditions ($p = 0.1$ MPa and $T = 300$ K with Nosé−Hoover thermostats and barostats with relaxation time constants of 1 and 4 ps, respectively) for 200 ps. Therefore, Gromacs simulations were performed using 2 fs timesteps and 2 nm cutoff distances, with Ewald summation corrections performed beyond the cutoffs. The isothermal-isobaric ensemble conditions used during equilibration were $p = 0.1$ MPa and $T = 300$ K with V-rescale thermostats and Berendsen barostats with relaxation time constants of 1 and 4 ps, respectively. After 10 ns, the density of each system reached constant and consistent values, indicating that equilibrium had been attained and possible ergodicity problems had been overcome. Finally, at least six consecutive production stages of 1.0 ns each were performed using 1 fs timestep, the isothermal-isobaric ensemble conditions used during equilibration were $p = 0.1$ MPa and $T = 300$ K with Nosé−Hoover thermostats and Parrinello-Rahman barostats with relaxation time constants of 1 and 4 ps, respectively. The combined results were used for the aggregation analyses of all studied ionic liquids (see below).

The aggregation analyses of the $[C_2C_1Im][C_1F_3SO_3]$, $[C_2C_1Im][C_2F_4SO_3]$, $[C_2C_1Im][C_4F_9SO_3]$, $[C_2C_1Im][C_8F_{17}SO_3]$, $[C_2C_1Im][C_1SO_3]$, $[C_2C_1Im][C_4H_9SO_3]$, $[C_2C_1Im][C_1CO_2]$ and $[C_2C_1Im][C_1F_3CO_2]$ ionic liquids and their mixtures with water focused on three types of issues: (i) the evaluation of the connectivity between the charged moieties of the molecular ions that compose the so-called polar network; (ii) the evaluation of the connectivity within the water and an estimation of the corresponding aggregate size; and (iii) the evaluation of the connectivity between the anion of the ionic liquids and water. The connectivity analyses are based on algorithms[S17-S19] previously described based on neighbour lists and interaction distance criteria, adapted to take into account the interaction centres of the different species.

The ILs colour code in Fig. 3 and 4 of the manuscript is: red (negative charges) and blue (positive charges) segments represent the interactions from the polar network of the two ions; grey space-filled areas represent the domains caused by the hydrogenated side chains; while the groups of green spheres illustrate the perfluoroalkyl apolar domains. Please note that the polar part includes the first methylene/methyl or fluorinated methylene groups directly connected to the imidazolium ring or the sulfonate/carboxylate moiety. This means that $[C_1C_1Im]^+$ would be all blue and $[C_1F_3SO_3]^-$ is all red. In other words, the gray/green colour code only applies to alkyl/perfluorinated alkyl chains from the β carbon onwards.

Table S3. Simulation conditions, size of the equilibrated boxes and concentrations.

	System	$wt_{IL}\%$	n_{IL}	n_w	l_{box} nm	V_{box} nm^3
1	[C$_2$C$_1$Im][C$_1$F$_3$SO$_3$] + water	30	100	3300	5.568	127.7
2	[C$_2$C$_1$Im][C$_1$F$_3$SO$_3$] + water	50	180	2600	5.080	131.1
3	[C$_2$C$_1$Im][C$_1$F$_3$SO$_3$] + water	90	390	620	5.158	137.2
4	[C$_2$C$_1$Im][C$_2$F$_4$SO$_3$] + water	30	88	3300	5.035	127.6
5	[C$_2$C$_1$Im][C$_2$F$_4$SO$_3$] + water	50	165	2600	5.109	133.4
6	[C$_2$C$_1$Im][C$_2$F$_4$SO$_3$] + water	90	350	620	5.179	138.9
7	[C$_2$C$_1$Im][C$_4$F$_9$SO$_3$] + water	30	62	3300	4.983	123.7
8	[C$_2$C$_1$Im][C$_4$F$_9$SO$_3$] + water	50	115	2600	5.009	125.7
9	[C$_2$C$_1$Im][C$_4$F$_9$SO$_3$] + water	90	250	620	4.999	124.9
10	[C$_2$C$_1$Im][C$_8$F$_{17}$SO$_3$] + water	30	43	3300	4.969	122.7
11	[C$_2$C$_1$Im][C$_8$F$_{17}$SO$_3$] + water	50	78	2600	4.967	122.6
12	[C$_2$C$_1$Im][C$_8$F$_{17}$SO$_3$] + water	90	180	620	4.988	124.1
13	[C$_2$C$_1$Im][C$_1$SO$_3$] + water	30	125	3300	5.106	133.1
14	[C$_2$C$_1$Im][C$_1$SO$_3$] + water	50	230	2600	5.218	142.1
15	[C$_2$C$_1$Im][C$_1$SO$_3$] + water	90	490	620	5.422	159.4
16	[C$_2$C$_1$Im][C$_4$H$_9$SO$_3$] + water	30	105	3300	5.135	135.4
17	[C$_2$C$_1$Im][C$_4$H$_9$SO$_3$] + water	50	190	2600	5.261	145.6
18	[C$_2$C$_1$Im][C$_4$H$_9$SO$_3$] + water	90	420	620	5.573	173.1
19	[C$_2$C$_1$Im][C$_1$CO$_2$] + water	30	150	3300	5.112	133.6
20	[C$_2$C$_1$Im][C$_1$CO$_2$] + water	50	280	2600	5.249	144.6
21	[C$_2$C$_1$Im][C$_1$CO$_2$] + water	90	600	620	5.560	171.8
22	[C$_2$C$_1$Im][C$_1$F$_3$CO$_2$] + water	30	115	3300	5.054	129.1
23	[C$_2$C$_1$Im][C$_1$F$_3$CO$_2$] + water	50	210	2600	5.127	134.8
24	[C$_2$C$_1$Im][C$_1$F$_3$CO$_2$] + water	90	450	620	5.267	146.1
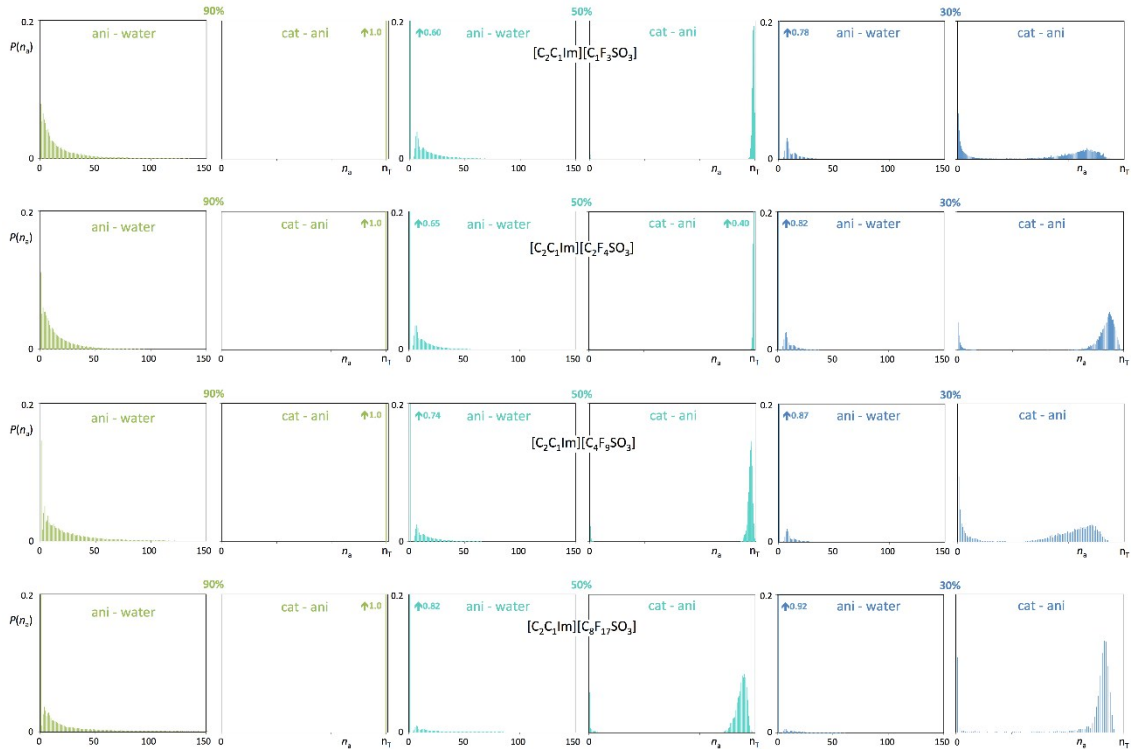
Fig. S6 Discrete probability distribution functions of water aggregate sizes, P(na), for different compositions of water-IL mixtures.
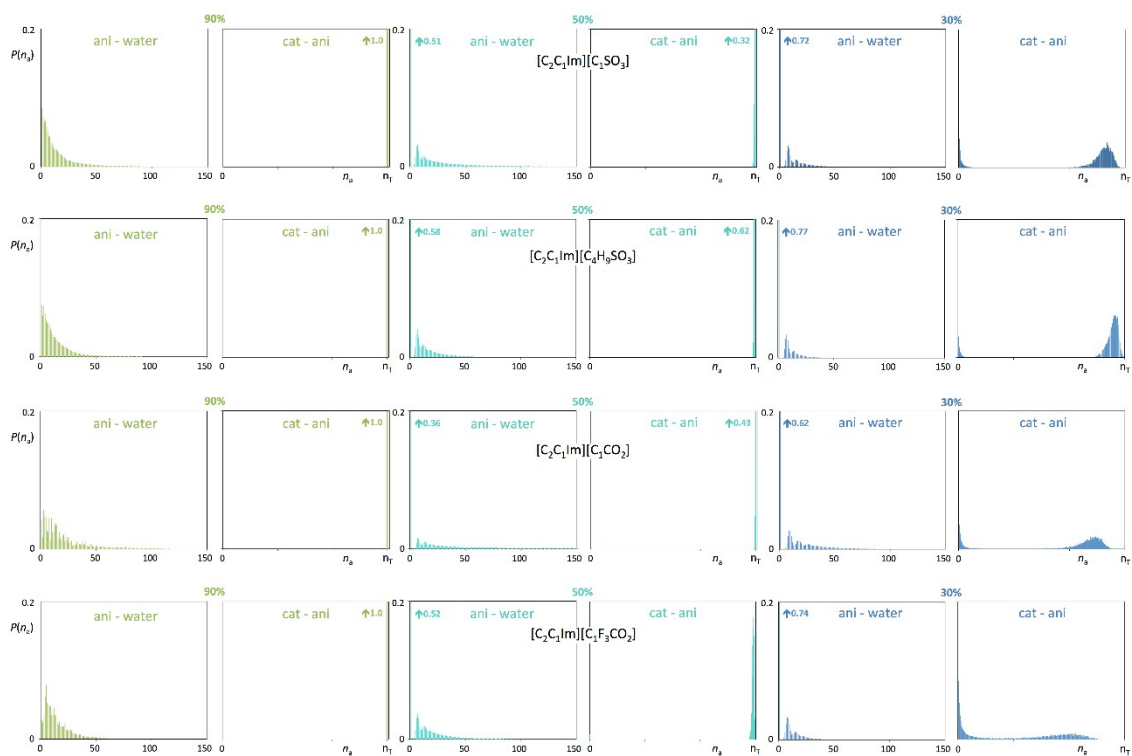
Fig. S7 Discrete probability distribution functions of water aggregate sizes, P(na), for different compositions of water-IL mixtures.
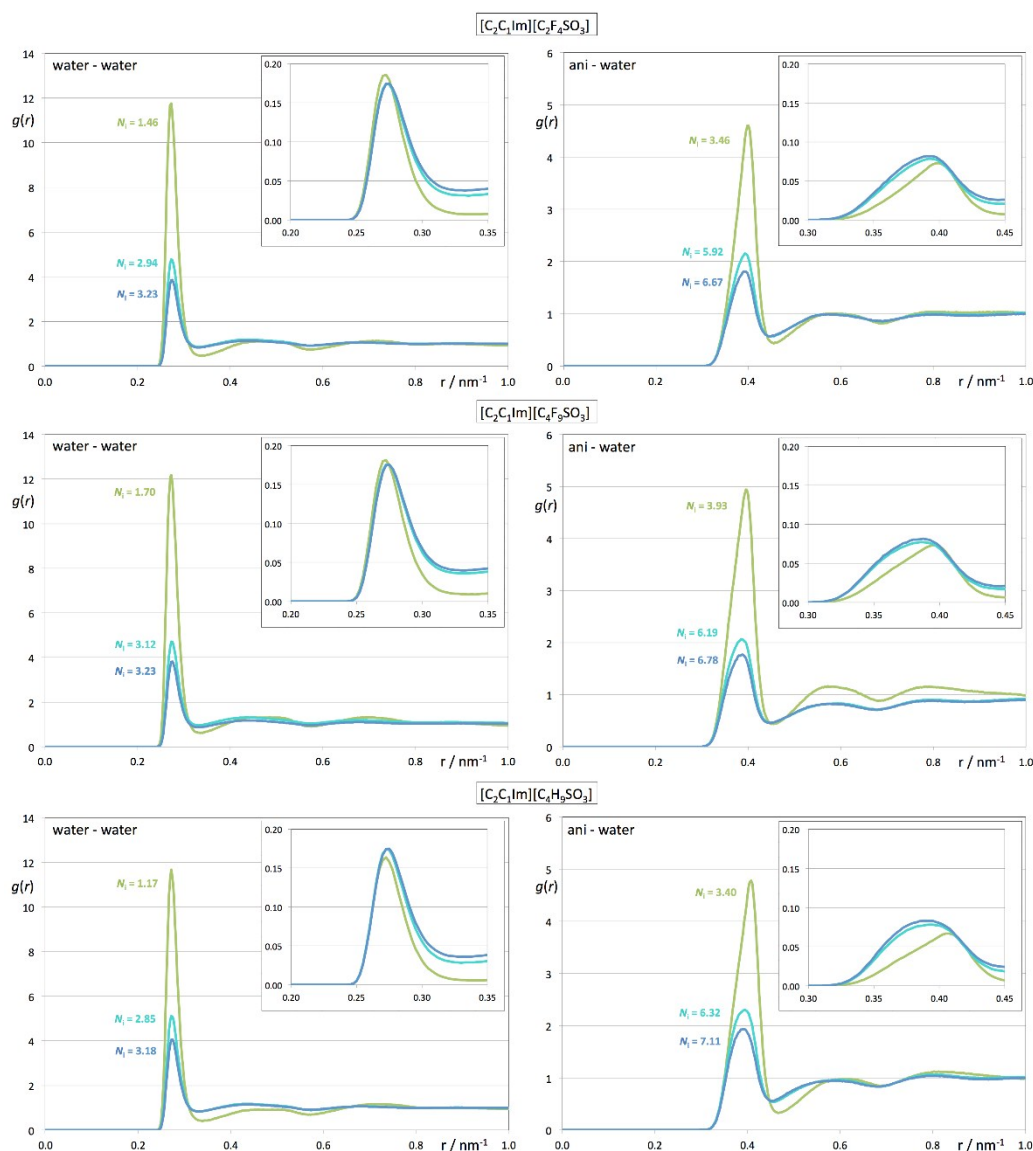
Fig. S8 Pair radial distribution functions, $g(r)$, between oxygen atoms in water (left column), and between sulphur atoms in the anion and oxygen atoms in water (right column) for different compositions of water-IL mixtures (green, cyan and blue represent 90, 50 and 30 wt$_{IL}$% compositions, respectively). To have a fair comparison between the first peaks in the different water-IL mixtures, the RDFs were multiplied by the corresponding numerical density (inset). The average size of contact neighbours, N_i, in the water aggregates and anion-water aggregates are also presented in the figure and were calculated from the integration of the first peaks of the corresponding $g(r)$ functions.

Funding Sources

ACKNOWLEDGMENT

REFERENCES

(S1) N. S. M. Vieira, P. M. Reis, K. Shimizu, O. A. Cortes, I. M. Marrucho, J. M. M. Araújo, J. M. S. S. Esperança, J. N. C. Lopes, A. B. Pereiro and L. P. N. Rebelo, *RSC Adv*., 2015, **5**, 65337.

(S2) A. B. Pereiro, J. M. M. Araújo, F. S. Teixeira, I. M. Marrucho, M. M. Piñeiro and L. P. N. Rebelo, *Langmuir*, 2015, **31**, 1283.

(S3) M. A. Ab Rani, A. Brant, L. Crowhurst, A. Dolan, M. Lui, N. H. Hassan, J. P. Hallett, P. A. Hunt, H. Niedermeyer, J. M. Perez-Arlandis, M. Schrems, T. Welton, R. Wilding, *Phys. Chem. Chem. Phys*., 2011, **13**, 16831.

(S4) A. B. Pereiro, J. M. M. Araújo, F. S. Teixeira, I. M. Marrucho, M. M. Piñeiro and L. P. N. Rebelo, *Langmuir*, 2015, **31**, 1283.

(S5) C. Zhong, F. Cheng, Y. Zhu, Z. Gao, H. Jia and P. Wei, *Carbohydrate Polymers*, 2017, **174**, 400.

(S6) T. V. Doherty, M. Mora-Pale, S. E. Foley, R. J. Linhardt and, J. S. Dordick, *Green Chem*., 2010, **12**, 1967.

(S7) D. L. Minnick, R. A. Flores, M. R. DeStefano and A. M. Scurto, *J. Phys. Chem. B*, 2016, **120**, 7906.

(S8) M. Praprotnik, D. Janežič and J. Mavri, *J. Phys. Chem. A*, 2004, **108**, 11056.

(S9) J. N. Canongia Lopes, J. Deschamps and A. A. H. Pádua, *J. Phys. Chem. B*, 2004, **108**, 2038.

(S10) J. N. Canongia Lopes and A. A. H. Pádua, *J. Phys. Chem. B*, 2004, **108**, 16893.

(S11) J. N. Canongia Lopes, A. A. H. Pádua and K. Shimizu, *J. Phys. Chem. B*, 2008, **112**, 5039.

(S12) Smith, W.; Forester, T. R. The DL_POLY Package of Molecular Simulation Routines (v.2.2); The Council for The Central Laboratory of Research Councils. Warrington: Daresbury Laboratory, 2006.

(S13) H. J. C. Berendsen, D. van der Spoel and R. van Drunen, Comput, *Phys. Commun*., 1995, **91**, 43.

(S14) S. Páll, M. J. Abraham, C. Kutzner, B. Hess and E. Lindahl, in Solving Software Challenges for Exascale. Vol. 8759, Springer, Cham, 2015, pp. 3–27.

(S15) M. J. Abraham, T. Murtola, R. Schulz, S. Páll, J. C. Smith, B. Hess and E. Lindahl, SoftwareX, 2015, **1-2**, 19.

(S16) L. Martínez, R. Andrade, E. G. Birgin and J. M. Martínez*, J. Comput. Chem*., 2009, **30**, 2157.

(S17) A. F. M. Claudio, M. C. Neves, K. Shimizu, J. N. Canongia Lopes, M. G. Freire and J. A. P. Coutinho, *Green Chem*., 2015, **17**, 3948.

(S18) K. Shimizu, C. E. S. Bernardes and J. N. Canongia Lopes, *J. Phys. Chem. B*, 2014, **118**, 567.

(S19) C. E. S. Bernardes, K. Shimizu, A. I. M. C. Lobo Ferreira, L. M. N. B. F. Santos and J. N. Canongia, *J. Phys. Chem. B*, 2014, **118**, 6885.